

## Surface integrity investigation of ground ceramic workpieces for biomedical applications

Pablo Fook<sup>1</sup>, Oltmann Riemer<sup>1</sup>, Bernhard Karpuschewski<sup>1</sup>

<sup>1</sup> Laboratory for Precision Machining (LFM), Leibniz Institute for Materials Engineering (IWT), MAPEX Center for Materials and Processes, University of Bremen, Germany

[fook@iwt.uni-bremen.de](mailto:fook@iwt.uni-bremen.de)

### Abstract

Traditionally, metallic materials were the only option for both medical and dental treatments. This setting has been changed in the last decades once the interest in ceramic implants renewed with the development of biomaterials science and ductile mode manufacturing. In addition, it has been reported that patients with a metal implant can show allergic reactions. This work aims to determine the influence of various micro-grinding parameters on the surface and subsurface damage for two typical bioceramic material, i.e. zirconia (ZrO<sub>2</sub>) and zirconia toughened alumina (ZTA). In this regard, the specimens are machined with ultrasonic vibration assisted grinding (UVAG) following the same machining parameters and two abrasive tools with different diamond grain sizes ( $d_g = 25$  and  $64 \mu\text{m}$ ). Herein, the processes are monitored through forces measurement. After micro-grinding, the surface roughness is assessed by White Light Interferometry (WLI), the microstructure is evaluated with a Scanning Electron Microscope (SEM), the flexural strength is measured by 3-point bending tests and residual stresses are quantified through X-Ray Diffraction (XRD). An increase of the flexural strength and compressive residual stresses of ground ZrO<sub>2</sub> and ZTA workpieces were observed in comparison to as-received specimens. Those characteristics are indicating an improvement regarding the fatigue strength and fatigue life of the bioceramic materials. Although the surface roughness values of the ground bioceramics increased, the finished parts are in the specification for certain biomedical uses like dental implants. Based on these results, a relationship between the micro-grinding process and material behaviour can be established allowing understanding the mechanisms influencing ceramic materials due to the machining process.

Micro-grinding, surface integrity, bioceramic materials.

### 1. Introduction

Metallic implants were the only option for biomedical applications for decades [1, 2]. However, in recent years, it has been reported that corrosion and deterioration without wear enable metal ions to diffuse, which possibly lead to an allergic inflammatory response. Consequently, technical ceramics have become an accessible material alternative due to their broad spectrum of applications and combinations, e.g. biocompatibility, low plaque affinity and particular mechanical properties like high flexural strength [3, 4]. The use of ceramics for biomedical applications and the increasing development of computer-aided design and computer-aided manufacturing (CAD-CAM) technologies seem to be mutually accelerating trends [4]. Ultrasonic vibration assisted grinding (UVAG) is a material removal process that combines conventional diamond grinding and ultrasonic machining with an outstanding performance in order to improve the micro-grinding process of brittle materials, like ceramics [5]. In this study, the UVAG response in two types of bioceramic materials was characterised by monitoring the forces applied in the process and measuring the surface integrity of the as-received and ground workpieces.

### 2. Experimental setup

#### 2.1. Process kinematics

UVAG experiments were performed on an Ultrasonic 20 linear (DMG Mori GmbH, Germany), a five-axis machine tool.

The process kinematics and the resultant feed direction are illustrated in Figure 1 is a combination of the impact-like material removal of ultrasonic assisted lapping and the high efficiency of grinding with bound abrasive diamond grains along the ceramic workpiece.

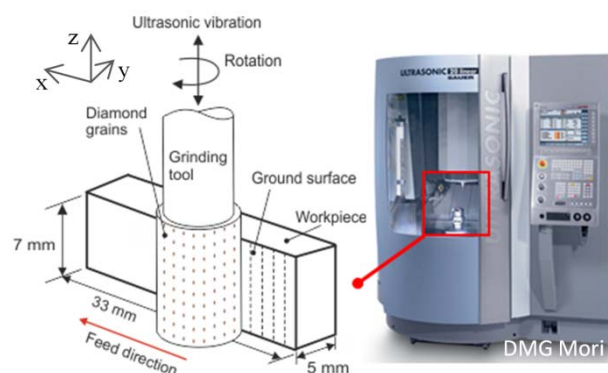


**Figure 1.** Setup of the UVAG process performed on a five-axis machine tool in this research.

For this investigation, diamond hollow drills of 10 mm diameter and natural diamond as abrasive grain with galvanic coated layer and average grain size ( $d_g$ ) of  $25 \mu\text{m}$  (D25) and  $64 \mu\text{m}$  (D64) are used.

The ceramic workpieces were ground in the x-direction using two grinding steps with each tool, i.e., D25 and D64. The machining conditions summarised in Table 1 were selected based on a screening campaign and a literature review [3-8]. Basically, in order to compare the machining conditions

regarding the grain size effect of the grinding tools, the same parameters (relative velocity, feed speed and rotation) are applied in both machining steps and the depth of cut ( $a_e$ ) are varied. The first grinding step was used for coarse grinding  $a_e = 10 \mu\text{m}$ , and subsequently, the second grinding was applied for finishing  $a_e = 5 \mu\text{m}$ . This strategy is used to achieve higher removal rates and low tool wear as well as reduce the possible effects of subsurface damage. After both procedures along the length direction, the workpiece was turned  $180^\circ$  to perform the same grinding conditions due to the requirements of the flexural bending tests where both faces should exhibit the same surface state.

**Table 1** Grinding conditions applied

Grinding step	Rel. velocity $V_{rel}$ (m/min)	Feed speed $V_f$ (mm/min)	Rotation (RPM)	Depth of cut $a_e$ ( $\mu\text{m}$ )
1 <sup>st</sup>	141	60	4500	10
2 <sup>nd</sup>				5

Moreover, five workpieces of each material were subjected to the same procedure due to statistical purposes. The process was performed under cooling with a water-based lubricant and the ultrasonic generator was excited at an approximate frequency of 20 kHz in all conditions.

After that, the group of workpieces ground with the tool D25 are named Process A ( $P_a$ ), and the specimens machined with the tool D64 are entitled Process B ( $P_b$ ).

## 2.2. Material properties

The ceramic workpieces (dims.  $5.0 \times 7.0 \times 33.0 \text{ mm}^3$ ) under investigation are fully sintered, partially machined, and commercially available tetragonal polycrystalline zirconia (TPZ), also known as zirconium dioxide ( $\text{ZrO}_2$ ) or zirconia, and zirconia toughened alumina (ZTA). These materials are zirconium-based ceramics and have intrinsic toughening mechanisms but differ in their mechanical properties [9], as shown in Table 2.

**Table 2** Description of the material properties [4]

Material	Density ( $\text{g/cm}^3$ )	Fracture toughness $K_{Ic}$ ( $\text{MPa m}^{1/2}$ )	Young's modulus (GPa)	Hardness (GPa)
$\text{ZrO}_2$	6.03	4.8	200	11
ZTA	4.10	8	380	16

## 2.3. Process monitoring - Force measurement

A three-component force dynamometer unit (Kistler 9256-C2) is used for the measurement of the grinding forces. A data acquisition and analysis system (MesUSoft 2.5.23) is used for data collection and display. Herein, this study focused on the forces applied to the y-direction as a methodology to monitor the machining process. The mean normal force ( $F_\theta$ ) is estimated according to average values of the maximum ( $F_{max}$ ) and minimum ( $F_{min}$ ) forces of each grinding step as illustrated in Figure 2.

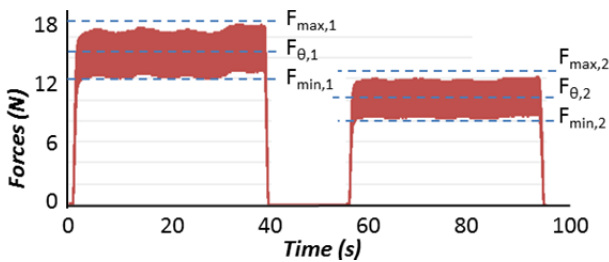


**Figure 2.** Illustration of the methodology used to evaluate the mean forces in each grinding step.

## 2.4. Workpiece characterisation

### 2.4.1 Surface roughness

The surface roughness was measured by using a 3D White Light Interferometer Talysurf CCI HD (WLI Taylor Hobson, UK). The tests were performed within an air-conditioned laboratory, where the temperature is kept at  $20^\circ\text{C}$  to analyse the  $\text{ZrO}_2$  and ZTA (as-received and ground) workpieces. The data were acquired under Gaussian filter with a specified cut off  $\lambda_c$  of 0.08 mm and a magnification of 20X.

### 2.4.2 Microstructure

The microstructure of the machined work specimens has been analysed to understand the different mechanisms of material removal from the work surface of the ceramics using a Scanning Electron Microscope (SEM). Hence, the material microstructure and surface topography of the ground workpieces were studied by means of a SEM Tabletop Microscope TM3030 (Hitachi Ltd, Japan) under a magnification of 300x.

### 2.4.3 Mechanical test

In order to evaluate the flexural strength of the workpieces, a 3-point bending test under a loading speed of 1 mm/min was applied on 5 workpieces of each batch as proposed in the literature [10,11] and the ASTM C1161 - 02c (Standard Test Method for Flexural Strength of Advanced Ceramics at Ambient Temperature). The tests were performed in universal ProLine testing machine Z005 (Zwick Roell AG, Germany) in which the loading force is applied by means of a loading pin with a distance between them equal to the supporting pins as illustrated in Figure 3. Herein, Weibull distribution was used to describe the strength of the tested samples. In this matter, the flexural strength and the Weibull modulus were determined with the maximum likelihood estimation [12].

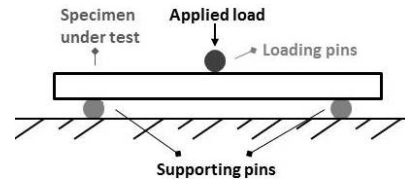


**Figure 3.** Schematic illustration of the 3-point bending test configuration

### 2.4.4 Residual stresses

In order to analyze the residual stress state based on X-ray pattern analysis, an X-Ray Diffraction (XRD) machine (Bruker Co., Germany) was used to perform the measurements along the diagonal stress axis (Cu  $K\alpha$ -source, 30 kV and 40 mA radiation) of as-received and ground ceramic specimens.

## 3. Results and Discussion

Table 3 shows the average values of each group of the bioceramic specimens and machining conditions according to the methodology mentioned in section 2.3. Due to the smaller depths of cut on the second grinding, lower forces are also measured in  $F_{\theta,2}$  for all conditions in comparison to the first machining step, i.e., the forces in  $F_{\theta,1}$ . In general, lower forces are beneficial for the tool wear and tool life [3-5]. Specifically for the machining of zirconia, Process A ( $P_a$ ) revealed higher force values in both grinding steps in regard to Process B ( $P_b$ ). However, the forces measured during the machining of ZTA workpieces show no significant differences between  $P_a$  and  $P_b$ .

**Table 3** Mean forces in the grinding processes

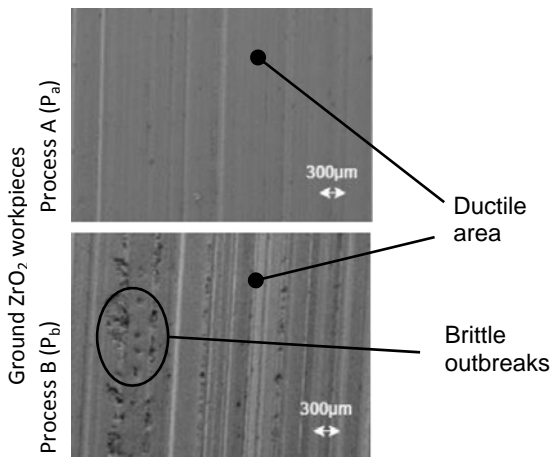
Material	Condition	Forces (N)	
		1 <sup>st</sup> step $F_{\theta,1}$	2 <sup>nd</sup> step $F_{\theta,2}$
ZrO <sub>2</sub>	Ground - P <sub>a</sub>	13.4 ± 0.4	10.9 ± 0.9
	Ground - P <sub>b</sub>	11.3 ± 0.2	8,1 ± 0.1
ZTA	Ground - P <sub>a</sub>	12.3 ± 0.5	9,5 ± 0.4
	Ground - P <sub>b</sub>	13.2 ± 0.7	9.4 ± 0.4

Table 4 shows the surface roughness values Sa (arithmetical mean height) of the as-received and ground ZrO<sub>2</sub> and ZTA specimens. Although the surface roughness increased considerably due to the machining conditions for both materials, the values of the conditions P<sub>b</sub> are considered optimum results for specific biomedical uses, like dental implants suggested to exhibit a surface roughness Sa between 500 to 1000 nm [13].

**Table 4** The surface roughness of the workpieces

Material	Condition	Sa (nm)
ZrO <sub>2</sub>	As-received	308.0 ± 5.8
	Ground - P <sub>a</sub>	319.5 ± 21.7
	Ground - P <sub>b</sub>	889.0 ± 94.6
ZTA	As-received	314.5 ± 7.6
	Ground - P <sub>a</sub>	367.6 ± 18.4
	Ground - P <sub>b</sub>	669.0 ± 52.7

In Figure 4 and Figure 5, SEM pictures of ground surfaces are shown as an analysis of the workpieces microstructure. In both figures, the surfaces show brittle intercrystalline breakouts, high roughness and ploughing at the scratch edges. Nevertheless, also this surface shows areas, where the material is removed in a more ductile way. Herein, zirconia ground workpieces showed a greater amount of ductile areas than ZTA specimens. The brittle outbreak marks are more visible in ZTA specimens which links to the higher hardness and of the material in comparison to ZrO<sub>2</sub> materials. This shows that the diamond grain sizes of the tools, respectively D25 for P<sub>a</sub> and D64 for P<sub>b</sub>, are influencing the surface topography for the same grinding parameters.



**Figure 4.** Surface topography and microstructure of ZrO<sub>2</sub> ground workpieces.

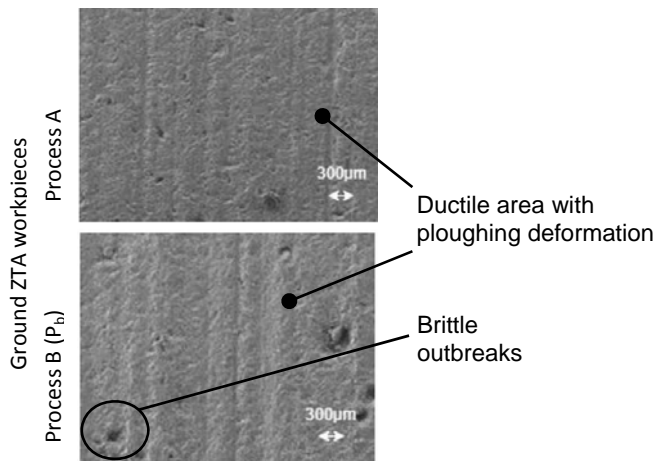


**Figure 5.** Surface topography and microstructure of ZTA ground workpieces.

Different mechanical response of the materials is observed after UVAG. An improvement of the flexural strength of the ground specimens is seen for zirconia specimens in regard to the as-received workpieces and the coarse grains of the grinding tools (P<sub>b</sub>) are beneficial for this behaviour – see Table 5. The increased strength of the workpieces due to grinding is associated with the toughening mechanisms in the ground surface of zirconium-based ceramics where the zirconia phase change the crystal structure from a tetragonal to a monoclinic structure. This transformation results in a 3 to 5 % volume change which compresses the microstructure of the material [14]. Conversely, a decrease in the Weibull modulus is detected. The decrease of the Weibull modulus shows worse reliability of the flexural tests and a broadened probability curve of the strength distributions [12, 14].

Although no differences are observed between the as-received and P<sub>b</sub> ground ZTA workpieces, a slight increase of the flexural strength of the specimens with P<sub>a</sub> is verified. Anyhow, the grinding parameters were beneficial to obtain a greater Weibull modulus for ZTA materials.

**Table 5** Results of the 3-point bending test

Material	Condition	Flexural strength (MPa)	Weibull modulus
ZrO <sub>2</sub>	As-received	863.4	19.9
	Ground - P <sub>a</sub>	904.3	12.7
	Ground - P <sub>b</sub>	990.4	11.3
ZTA	As-received	476.7	13.2
	Ground - P <sub>a</sub>	501.9	27.8
	Ground - P <sub>b</sub>	475.3	26.6

Analysis with X-Ray Diffraction (XRD) indicated an increase in the compressive residual stresses of the ground samples – see Figure 6. The ZrO<sub>2</sub> workpieces increased the compressive stresses from -64 MPa to -280 MPa for P<sub>a</sub> and -425 MPa for P<sub>b</sub> ground specimens. For ZTA samples, the residual stresses increased from -123 MPa to -152 MPa for P<sub>a</sub> and -199 MPa for P<sub>b</sub> machined workpieces. This phenomenon is due to the toughening mechanism which also involves the phase transformation already mentioned. In general, compressive values are likewise desired in the specimen surface for biomedical application. E.g. the compressive residual stress tends to increase fatigue strength and fatigue life of bioceramic materials [2,13].

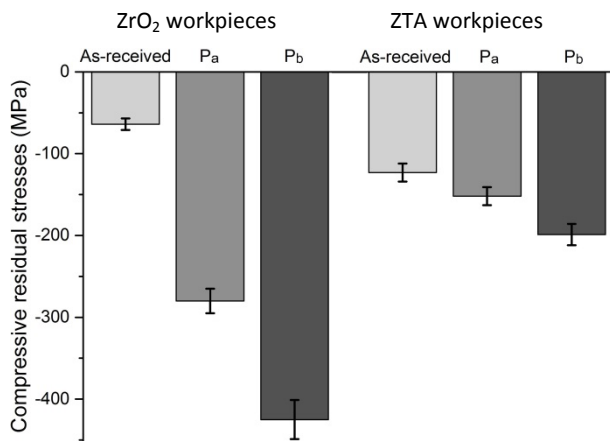


**Figure 6.** Residual stresses of the as-received and ground ZrO<sub>2</sub> and ZTA workpieces (machined with P<sub>a</sub> and P<sub>b</sub> conditions) measured through XRD technique.

#### 4. Conclusions and Outlook

Regarding the process monitoring, higher forces are measured in the first grinding step for all process conditions in comparison to the second machining step. Process A (P<sub>a</sub>) had higher force values in both grinding steps in regard the Process B (P<sub>b</sub>) for ZrO<sub>2</sub> materials. However, the forces measured during the machining of ZTA workpieces show no significant differences between P<sub>a</sub> and P<sub>b</sub>.

The surfaces were analysed through WLI and SEM measurements. Although the surface roughness values of the ground bioceramics became higher, the ground parts are suitable for certain biomedical applications. For example, the workpieces machined with P<sub>b</sub> are suitable for dental implants.

Concerning the mechanical properties, an increase of the flexural strength and compressive residual stresses of ground ZrO<sub>2</sub> workpieces were observed in comparison to the as-received specimens. Those characteristics are indicating an improvement regarding the fatigue strength and fatigue life of these bioceramics.

Although no significant changes on the flexural strength of the ground ZTA specimens were observed, a significant improved of the Weibull modulus and compressive residual stresses are highlighted.

The results are helpful to understand the bioceramic materials response under micro-grinding conditions as well as to set further machining investigations.

The next studies include the correlation of the compressive stress values through the quantification of the tetragonal and monoclinic zirconia phases via XRD analysis as well as Raman spectroscopy [15]. In this regard, the new research aims to investigate the phase transformation phenomenon as well as to consider the microstructure of the as-received and ground bioceramics presented in this work.

#### Acknowledgements

This research work was undertaken in the context of MICROMAN project. MICROMAN is a European Training Network supported by Horizon 2020, the EU Framework Programme for Research and Innovation (Project ID: 674801).

The authors would like to thank the Advanced Ceramics Group (University of Bremen) for the experiments supported with the bending tests.

The collaboration and technical support performed by SCHOTT Diamantwerkzeuge GmbH is also gratefully acknowledged.

#### References

- [1] Branemark PI 1983 Osseointegration and its experimental background. *J prosthet Dent.* **50** 399-410
- [2] Osman RB and Swain MV 2015 A critical review of dental implant materials with an emphasis on titanium versus zirconia *Materials* **8.3** 932-58
- [3] Denkena B, Breidenstein B, Busemann S and Lehr CM 2017 Impact of hard machining on zirconia based ceramics for dental applications *Procedia CIRP* **65** 248-52
- [4] Zeng WM, Li ZC, Pei ZJ and Treadwell C 2005 Experimental observation of tool wear in rotary ultrasonic machining of advanced ceramics. *International Journal of Machine Tools and Manufacture* **45(12-13)** 1468-73.
- [5] Xiao X, Zheng K, Liao W and Meng H 2016 Study on cutting force model in ultrasonic vibration assisted side grinding of zirconia ceramics *International Journal of Machine Tools and Manufacture* **104** 58-67
- [6] Fook P and Riemer O 2018 Characterisation of zirconia-based ceramics after micro-grinding. *Proceedings of the WCMNM* 175-178
- [7] Fook P, Flosky C and Riemer, O 2017 Process Fingerprint Concept of the Micro Grinding of Dental Ceramic Implants 8. *Kolloquium Mikroproduktion BIAS Verlag* 173-180
- [8] Fook P, Rickens K and Riemer O 2018. Surface and subsurface characterisation of bioceramic workpieces machined by micro-grinding. *Proceedings of the EUSPEN* **18** 463-464
- [9] Werkstoffe TKC. *TKC - Technische Keramik GmbH*. Access on 15.07.2018 by <http://tkc-keramik.de/downloads/datenblatt.pdf>
- [10] İşeri U, Özkurt Z, Kazazoğlu E and Küçüköğlü D 2010 Influence of grinding procedures on the flexural strength of zirconia ceramics. *Brazilian dental journal* **21.6** 528-532
- [11] Quinn J B and Quinn G D 2010 A practical and systematic review of Weibull statistics for reporting strengths of dental materials. *Dental Materials* **26.2** 135-147
- [12] Rockette H, Antle C and Klimko L A 1974 Maximum likelihood estimation with the Weibull model. *J. American Statistical Association* **69** 246-249
- [13] Gaviria L, Salcido J P, Guda T and Ong J L 2014 Current trends in dental implants. *Journal of the Korean Association of Oral and Maxillofacial Surgeons* **2** 50-60
- [14] Richerson D W 2005 Modern ceramic engineering: properties, processing, and use in design *CRC press*
- [15] Li M, Feng Z, Xiong G, Ying P, Xin, Q and Li, C 2001 Phase transformation in the surface region of zirconia detected by UV Raman spectroscopy. *The Journal of Physical Chemistry B* **105.34** 8107-8111.